This is a repository copy of *A billion or more years of possible periglacial/glacial cycling in Protonilus Mensae, Mars*.

White Rose Research Online URL for this paper:
https://eprints.whiterose.ac.uk/190383/

Version: Supplemental Material

Article:
Soare, R.J., Williams, J.-P., Hepburn, A.J. et al. (1 more author) (2022) A billion or more years of possible periglacial/glacial cycling in Protonilus Mensae, Mars. Icarus, 385. 115115. ISSN 0019-1035

https://doi.org/10.1016/j.icarus.2022.115115

© 2022 Elsevier Inc. This is an author produced version of a paper subsequently published in Icarus. Uploaded in accordance with the publisher's self-archiving policy. Article available under the terms of the CC-BY-NC-ND licence (https://creativecommons.org/licenses/by-nc-nd/4.0/).

Reuse
This article is distributed under the terms of the Creative Commons Attribution-NonCommercial-NoDerivs (CC BY-NC-ND) licence. This licence only allows you to download this work and share it with others as long as you credit the authors, but you can't change the article in any way or use it commercially. More information and the full terms of the licence here: https://creativecommons.org/licenses/

Takedown
If you consider content in White Rose Research Online to be in breach of UK law, please notify us by emailing eprints@whiterose.ac.uk including the URL of the record and the reason for the withdrawal request.

eprints@whiterose.ac.uk
https://eprints.whiterose.ac.uk/

FIGURES FOR:

A billion or more years of possible periglacial/glacial cycling in Protonilus Mensae, Mars

R.J. Soare,[1] J-P Williams,[2] A.J. Hepburn,[3] F.E.G. Butcher[4]

[1]Geography Department, Dawson College, Montreal, Qc, Canada, H3Z 1A4
(rsoare@dawsoncollege.qc.ca)

[2]Department of Earth, Planetary and Space Sciences, University of California, Los Angeles, CA, USA 90095

[3]Department of Geography, Durham University, Durham, United Kingdom DH1 3LE

[4]Department of Geography, University of Sheffield, Sheffield, United Kingdom S10 2TN

Final published version available at: Soare, R.J., Williams, J.-P., Hepburn, A.J., Butcher, F.E.G., 2022, A billion or more years of possible periglacial/glacial cycling in Protonilus Mensae, Mars, Icarus 385, 115115, https://doi.org/10.1016/j.icarus.2022.115115

Figure 1:

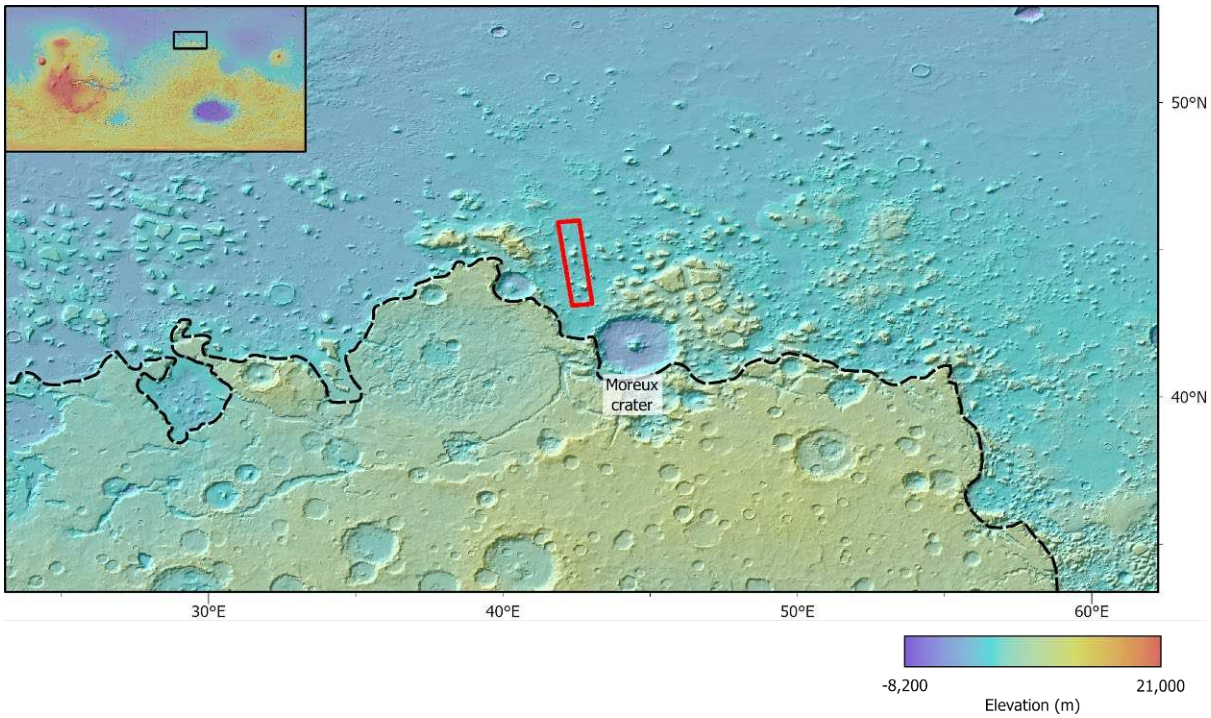

Fig. 1: The geographical footprint of our study area (red rectangle) in the *P*rotonilus *M*ensae [*PM*] region of Mars (extent shown by black box in inset of global elevation map of Mars). The black dashed-line highlights the Mars crustal dichotomy and the proximity of our footprint to it. Background colour comprises *MOLA* global-elevation (Zuber et al., 1992) in an equirectangular projection. *MOLA* data credit: *MOLA* Science Team, Arizona State University.

Figure 2

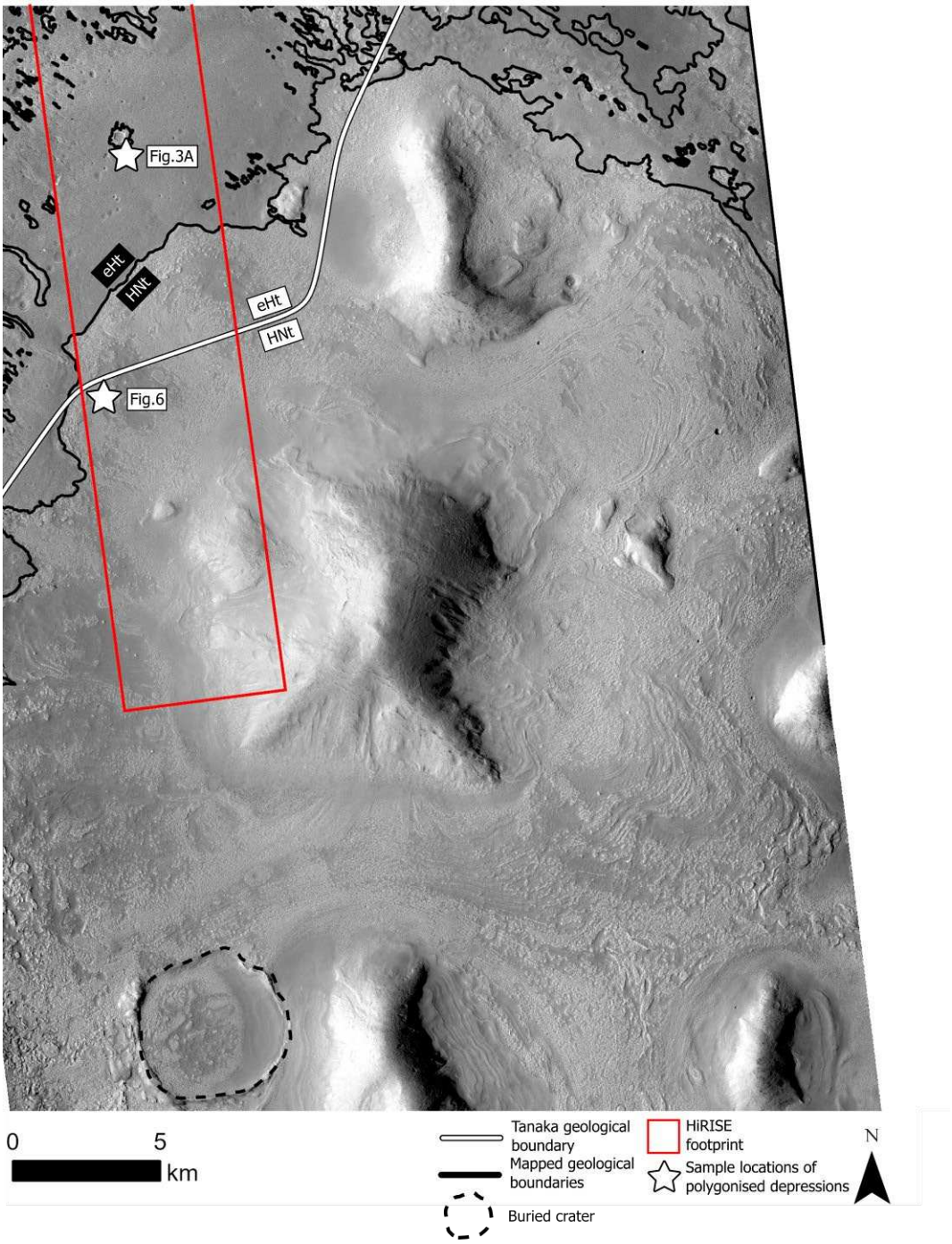

Fig. 2: C*TX* image F21_044083_2248_ XI_44N317W of geological units *eHt* and *HNt* in the *PM* region. The two units are separated by a contact first identified by Tanaka et al. (2014) and refined, here. The white line coincides with Tanaka's original boundary, derived of a large regional-scale map; the black line marks the updated contact. Age estimates of the large crater (serrated circle) suggest that it intercepts the floor of *HNt* at depth (Soare et al., 2022b). The red rectangle represents the footprint of *HiRISE* image ESP_028457_2255. Stars mark the sample locations of (candidate) clastically-sorted circles in unit *eHt* (see **Fig. 3a)** and polygonised but not clastically-sorted thermokarst-like depressions in unit *HNt* (see **Fig. 6)**. North is up. *CTX* image credit: *NASA/JPL*/Arizona State University. *HiRISE* image credit: *NASA/JPL*/University of Arizona.

Figure 3

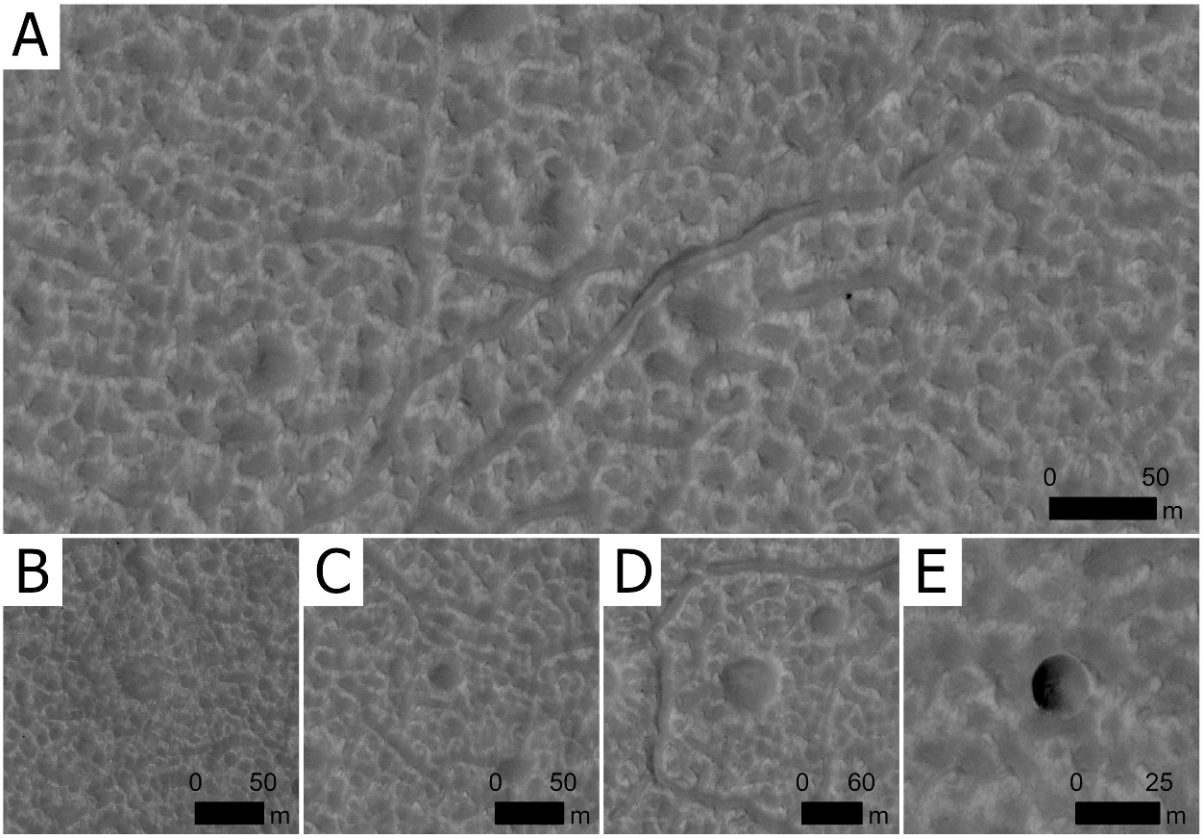

Fig. 3: a) Example of ubiquitous surface-coverage of unit *eHt* by decametre-scale circular to sub-circular or quasi-polygonised structures, elevated at the margins. The margins are punctuated by boulders and show a slightly lighter tone than the terrain circumscribed by them. *HiRISE* image ESP_028457_2255. Examples of four morphologic categories of depressions based on similarities to impact craters. **b)** *Type 0 - unlikely*: shallow, often irregular, or elliptical in shape with no apparent rim. **c)** *Type 1 - possible but ambiguous*: similar to *Type 0* but are circular in planform making them candidates for being impact related. **d)** *Type 2 - probable*: circular with uplifted rims and steeper interior wall slopes than typical of the surrounding depressions. **e)** *Type 3 - unambiguous*: bowl-shaped with sharp edges or rims and steep inward slopes. Scale bars are 20 m. North is up in all panels. *HiRISE* ESP_028457_2255. North is up in all panels. Image credit: *NASA*/*JPL*/University of Arizona.

Figure 4

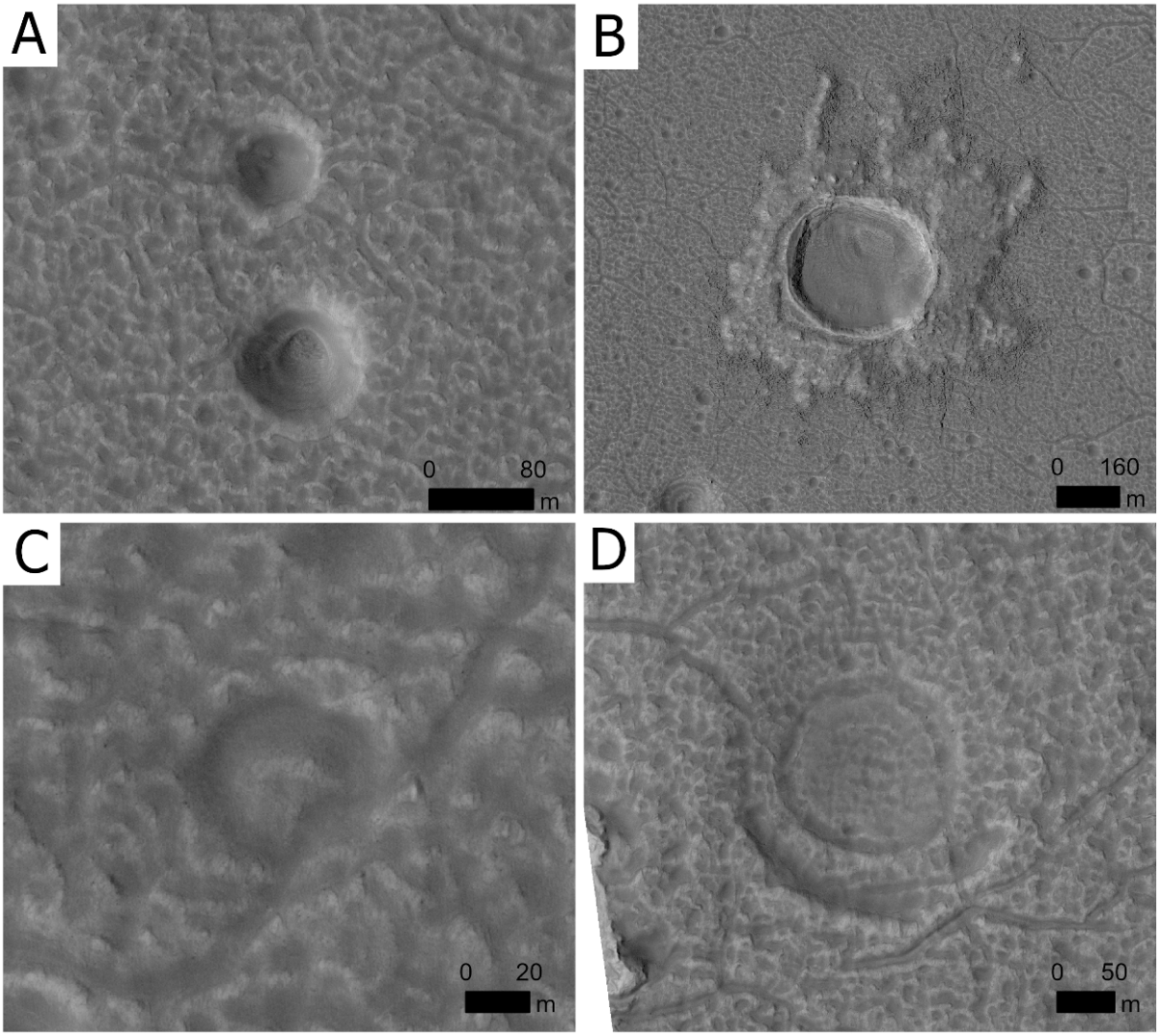

Fig. 4: a) Larger, unfilled bowl-shaped depressions confidently identified to be impact craters due to their size and depth. The lower crater is an example of a subset of these craters that have terraces in the interior wall outlining their center near the floor, possibly resulting from a transition in target properties. **b)** Largest crater (D = 350 m) identified in the count region with a clearly visible rim and surrounding ejecta material that appears to overlay the adjacent terrain. **c)** Example of a class of depressions with central mounds that may represent buried impact craters formed prior to the emplacement of the current exposed surface materials and could thus represent embedded craters exposed by exhumation. **d)** Class of subdued, shallow circular depressions with arcuate ridges, fractures, and scarps typically D > 100 m. These may represent ghost craters from a preexisting population of craters on an older underlying surface. North is up in all panels. *HiRISE* image ESP_028457_2255. Image credit: *NASA*/*JPL*/University of Arizona.

Figure 5:

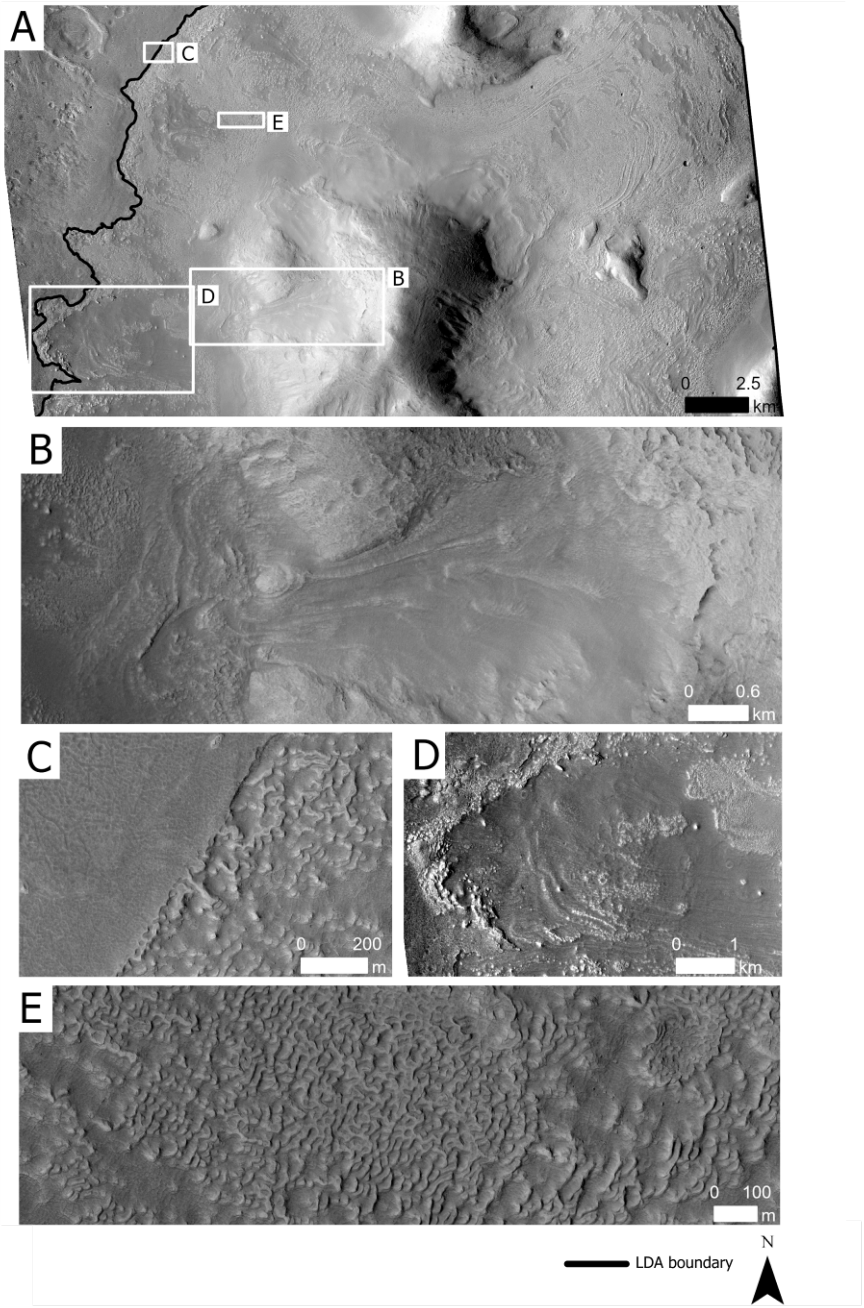

Fig. 5: a) Magnification of *CTX* (massifs-centred) context image. The black line demarcates the western margin of the principal *l*obate-*d*ebris *a*pron [*LDA*] in the image. **b)** Amphitheatre-shaped depression heading possible *VFFs* through a valley and towards a series of moraine-like ridges [*MLRs*] on the valley floor. Note possible medial *MLRs* in the midst of the *VFFs*. **c)** Degradational contact between the dark-toned terrain and the *LDA*. The degradational contact appears to have eroded backwards, revealing underlying textures consistent with the upper reaches of the *LDA*. **d)** A series of candidate push moraines associated with the alcove sourced glacier-like form. The possible moraines appear to pile up at the contact with unit *eHt* and the topographical profile of this location indicates that the former are at a higher elevation than the latter (see **Fig. 11a)**. This would be consistent with *CSFD*-based age estimates suggesting that unit *eHt* predates the light-toned surface of unit NHt. **e)** Small-sized ridge/trough assemblages that are open or closed, possibly formed by ablation and/or devolatilization and erosion.

Figure 6

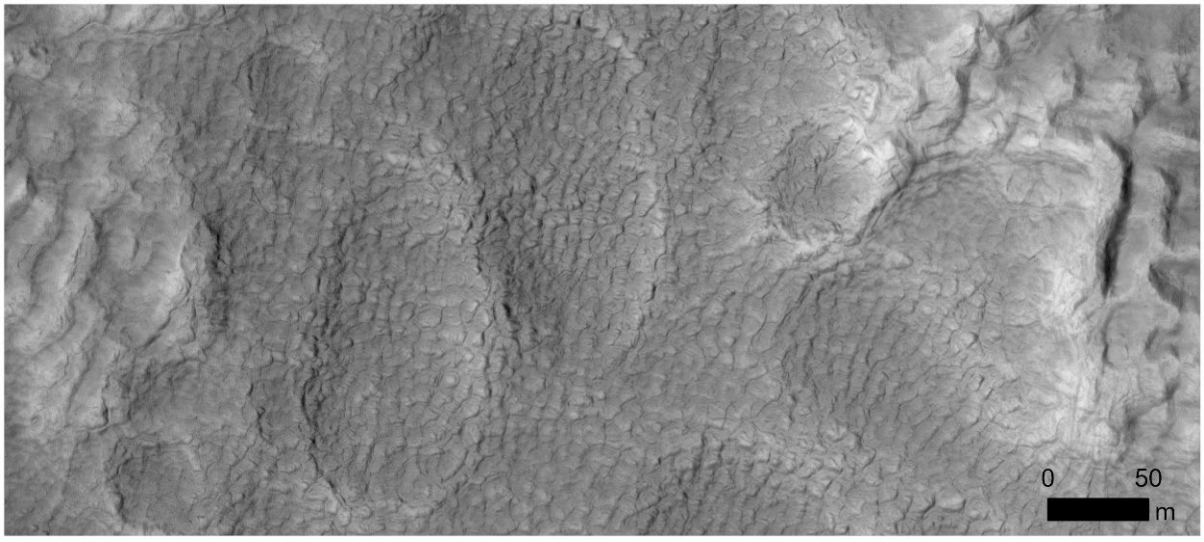

Fig. 6: Segment of light-toned terrain in which high-centred polygons and polygonised depressions occur. North is up. *HiRISE* Image credits: *NASA/JPL*/University of Arizona.

Figure 7

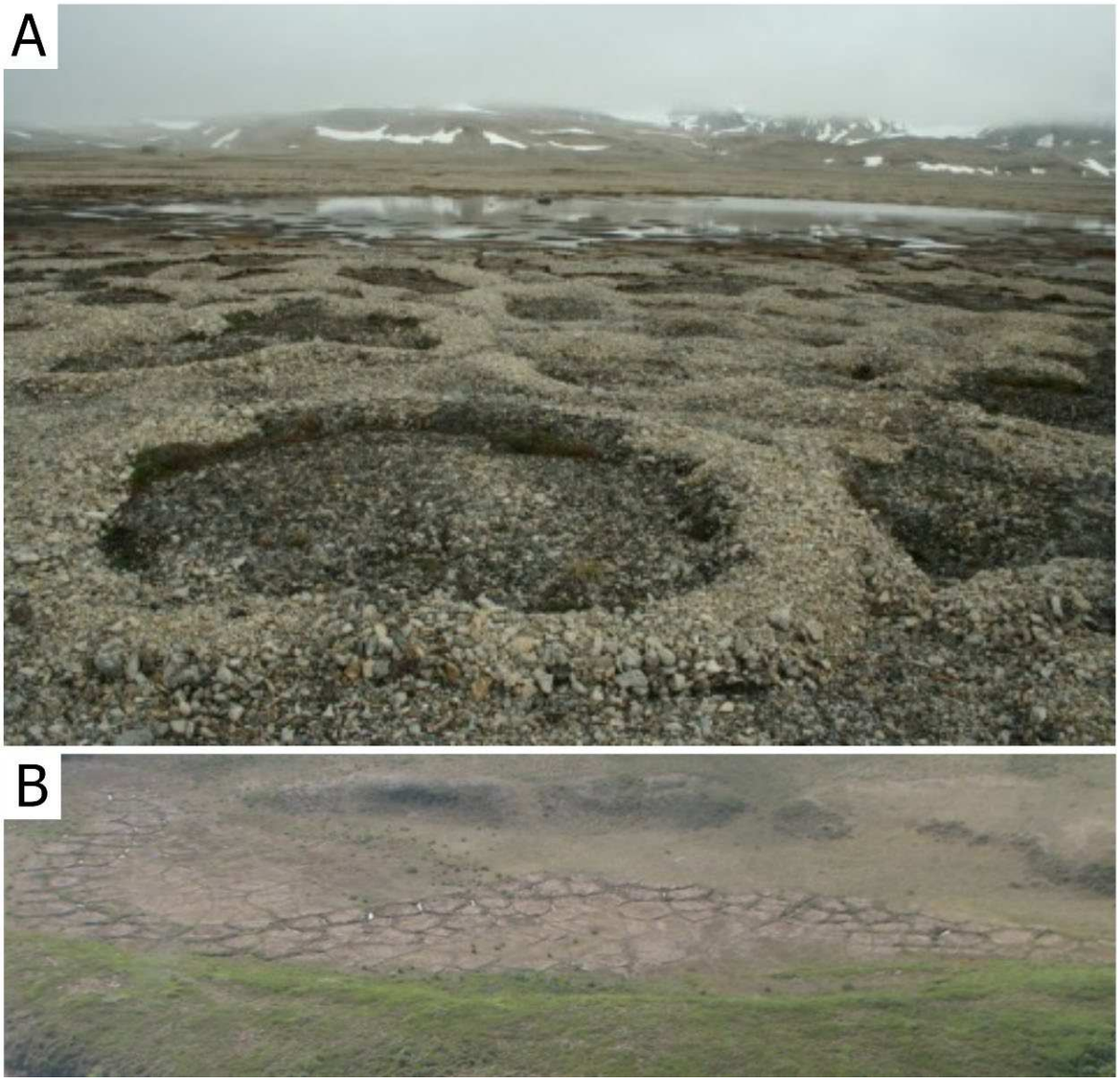

Fig. 7: a) Clastically-sorted circles, Kvadehukken, Svalbard. Photo credit and permission to reproduce granted: Ina Timling, Geophysical Institute, University of Alaska Fairbanks, 903 Koyukuk Drive, Fairbanks, Alaska, USA 99775). **b)** Oblique view of thermokarst-lake basin (alas) incised by polygons with centres slightly more elevated than the margins (Husky Lakes, midway between the coastal village of Tuktoyaktuk and Inuvik, on the eastern embankment of the Mackenzie River delta. Image credit: R. Soare.

Figure 8

Fig 8: a) Grosser Aletschgletscher glacier, Switzerland from the International Space Station (Image ISS013-E-77377) looking *NNE*. Labelled are the source cirque **(i)**, medial moraines generated as debris from adjoining basins coalesces **(ii)**, and a latero-frontal moraine marking the terminus of the glacier **(iii)**. **b)** Cwm Cau, a cirque on the eastern face of Cadair Idris, Wales. **c)** A 'degraded' glacial surface on Khumbu glacier, Nepal. Spatial heterogeneity in debris thickness leads to high local ablation where debris is thinnest and the subsequent development of ice cliffs and meltwater ponding (e.g., Watson et al., 2017). Panel **b)** and **c)** are reproduced with permission from https://www.swisseduc.ch/glaciers/, photo credit: M.J. Hambrey.

Figure 9

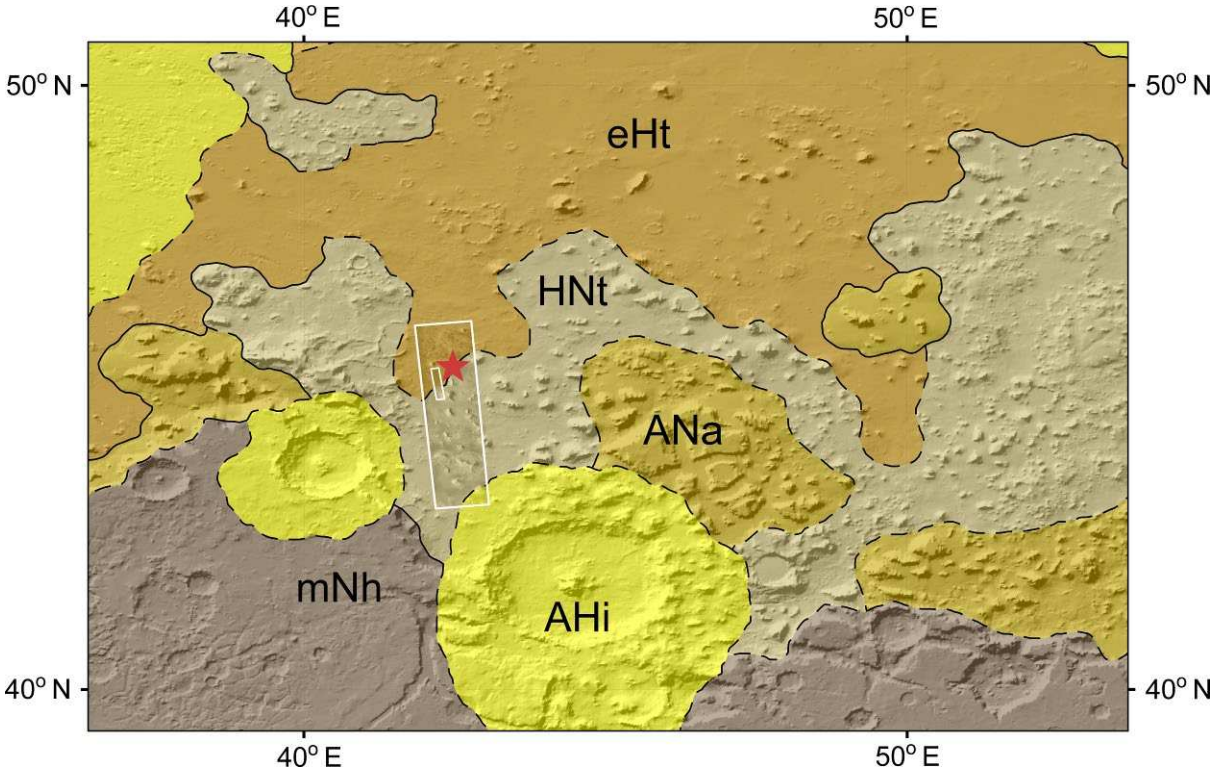

Fig. 9: Geologic units mapped by Tanaka et al (2014) centered on Protonilus Mensae and overlying *MOLA* shaded relief. Unit boundaries are marked with black lines, dashed where inferred. The larger white rectangle is the image boundary of *CTX* image F21_044083_2248_XI_44N317W; the smaller white rectangle is the image boundary of *HiRISE* image ESP_028457_2255. Red star marks the location of the topographical depression possibly exposing the basement of unit *eHt*. The relative elevation of the depression (see **Fig 11a)** is lower than the two other reference elevations for the dark and light-toned terrains at their geological contact immediately to the southwest **(Fig. 11a)**. Image credit *NASA/JPL*/Arizona State University.

Figure 10

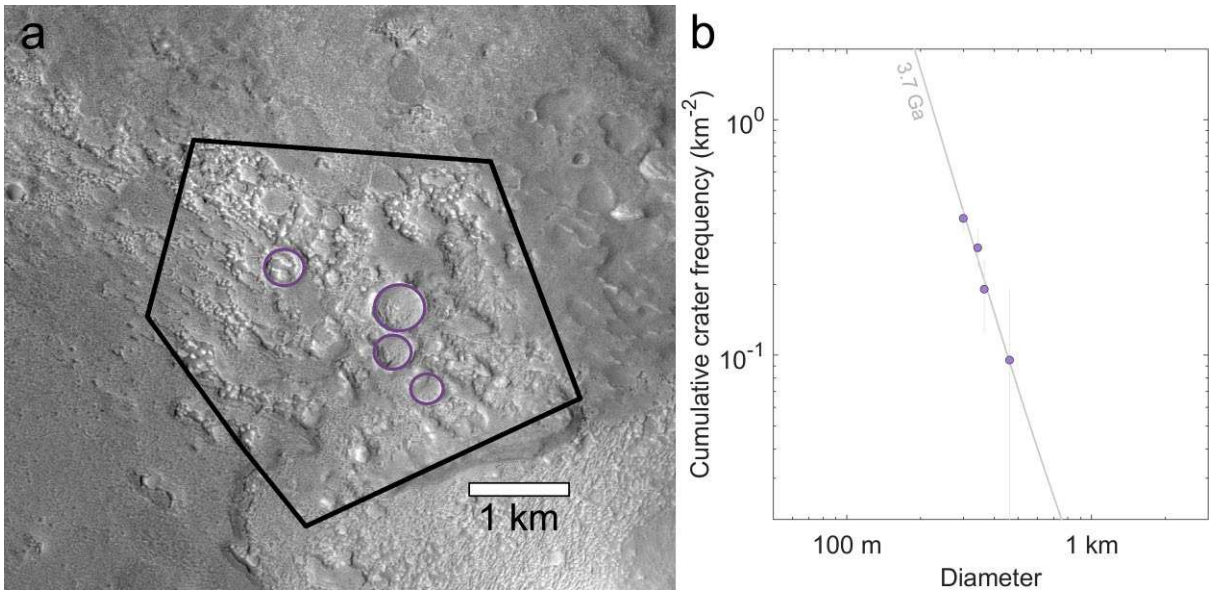

Fig. 10: a) Magnified *CTX* image of divot-like topographic depression (~10 km^2 area) referenced in **Fig. 9**. Four partially exposed craters $D \geq 300$ m (purple) are observed. **b)** The cumulative *CSFDs* for the craters compares well with a 3.7 Ga model isochron from Hartmann (2005) and with the age of the *eHt* unit identified by Tanaka et al., (2014).

Figure 11

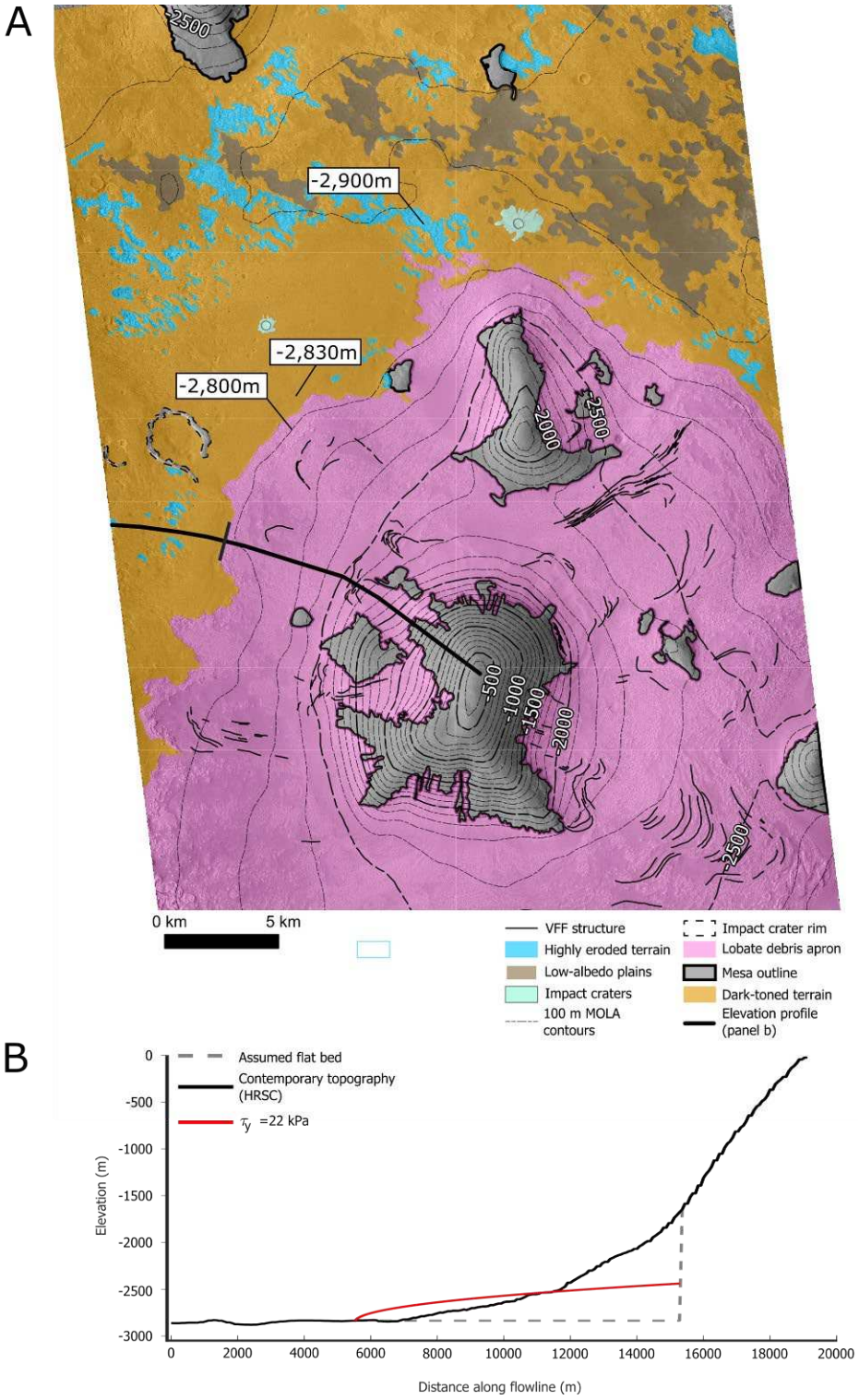

Fig. 11: a) Planimetric view and contour profile of units *HNt*/*eHt* based on *CTX* image. Contours derived from the global *MOLA* elevation dataset (Zuber et al., 1992). North is up. Image credit: *NASA/JPL/*Arizona State University. **b)** Modelled and measured surface profiles for the *VFF* shown in **a)**. Red line derived from 2D model of perfect plasticity, black line derived from *MOLA* elevation along the profile shown in **a)**. The modelled profile is a poor fit for the measured profile of the *VFF* and a thicker ice mass extending beyond the geological contact is predicted based upon our initial assumptions.

Figure 12

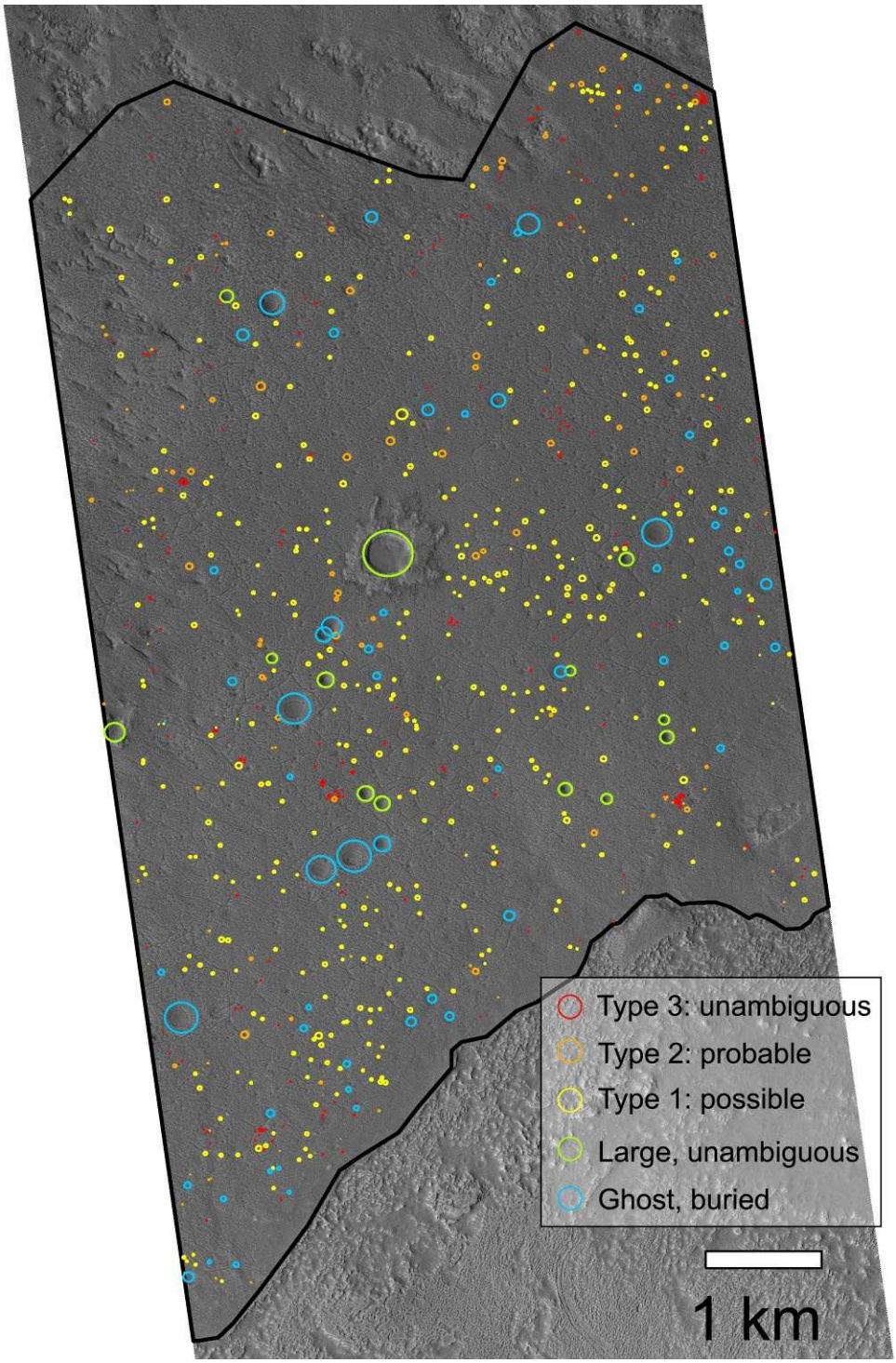

Fig. 12: Crater count area in (sample) segment of dark-toned terrain (outlined in black) (*HiRISE* image ESP_028457_2255). Crater colours indicate crater class: *red* -Type 3, *orange* - Type 2, *yellow* - Type 1, *green* - Large (D > 80 m), unfilled, *blue* - filled ghost/buried (see **Figs. 13**-**14**). Type 0 craters are excluded as their impact origin is highly uncertain. The Type 3, Type 2, and the large, unfilled craters represent a population of craters confidently identified as having accumulated on the surface of the lithic unit (*red*, *orange*, and *green* markers) and are used to generate the combined *CSFDs* in **Fig. 13**. Image credit: *NASA/JPL*/University of Arizona.

Figure 13

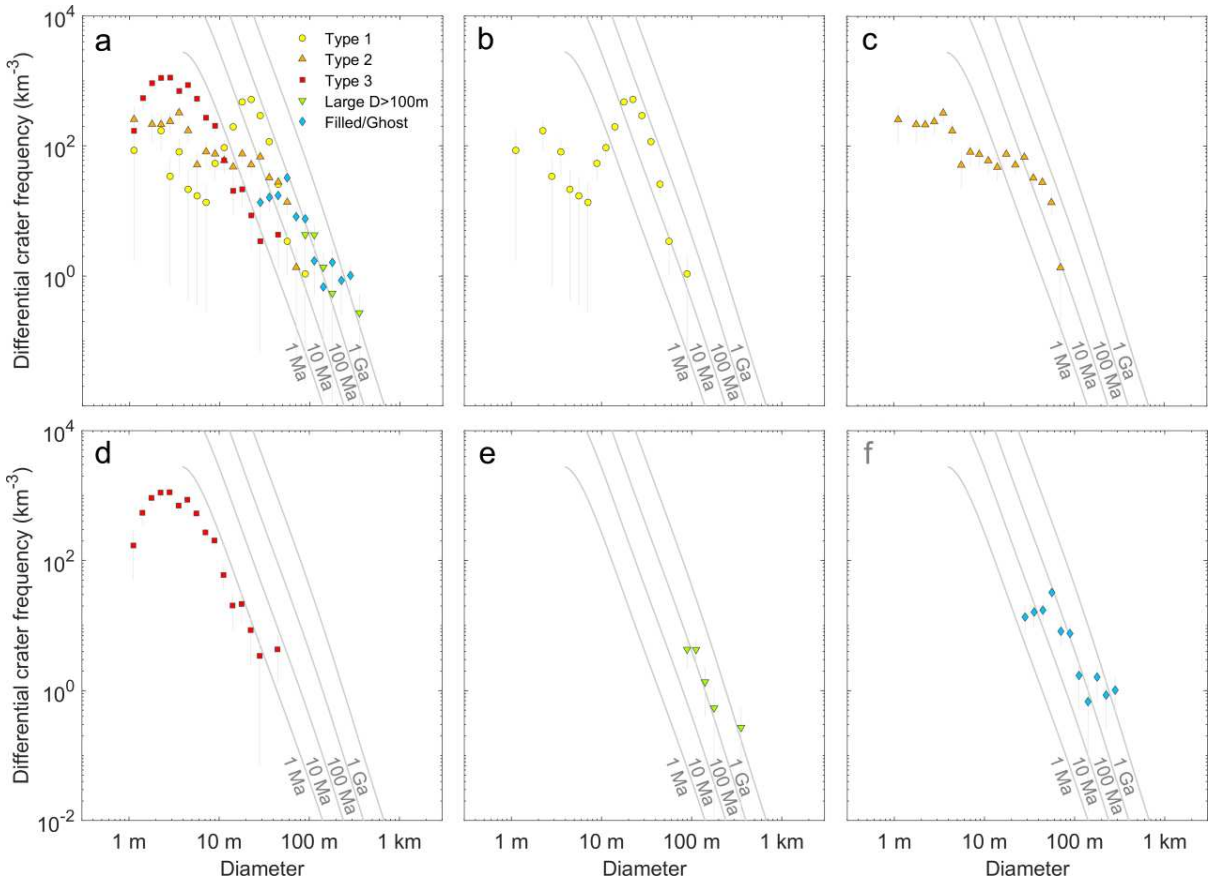

Fig. 13 a) Differential Crater Size-Frequency Distribution (*CSFD*) of each categorized crater class excluding *Type 0* because it is not deemed to be impact related. Marker colors correspond to colors of the mapped craters in **Fig. 12**. For clarity, **(b-f)** show the CSFDs individually: **b)** *Type 1*, **c)** *Type 2*, **d)** *Type 3*, **e)** *unfilled large D* ≳ 80 m, and **f)** *filled* (buried/ghost) craters. *Type 3* (*red*) craters represent smaller, fresh craters and suggest the upper surface has been stable for ~1 Myr against erosion and modification. *Type 2* craters are heavily modified but still visible after 10's of Myr. The larger unfilled craters (D > 80 m) suggest the material is at least ~100 Ma. The *CSFD* of the Type 1 craters *b)* peak at D ~ 10 - 40 m. Since the texture of the terrain occurs at this length-scale this could indicate that many of the features mapped as *Type 1* craters have been misidentified. Thus, this class of craters has been excluded in the combined isochrons in **Fig. 14**. Their exclusion makes little difference on the age interpretation. Model isochrons (gray) are for ~1 Ma, ~10 Ma, ~100 Ma, ~1 Ga for all figures.

Figure 14

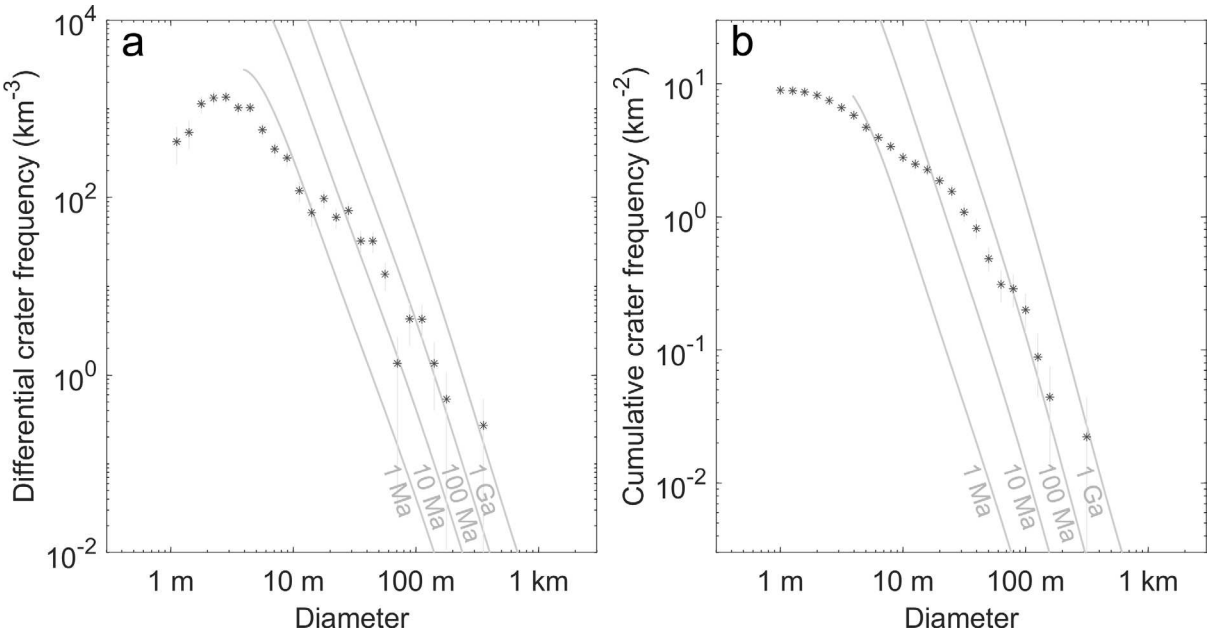

Fig. 14: a) Differential and **b)** cumulative *CSFDs* of the craters confidently interpreted as impact related in the dark-toned unit (*Types 2* and *3*, and the large unfilled craters from **Fig. 4a**. The largest craters (D > 80 m) suggest the dark-toned unit is >~100 Ma.

Figure 15

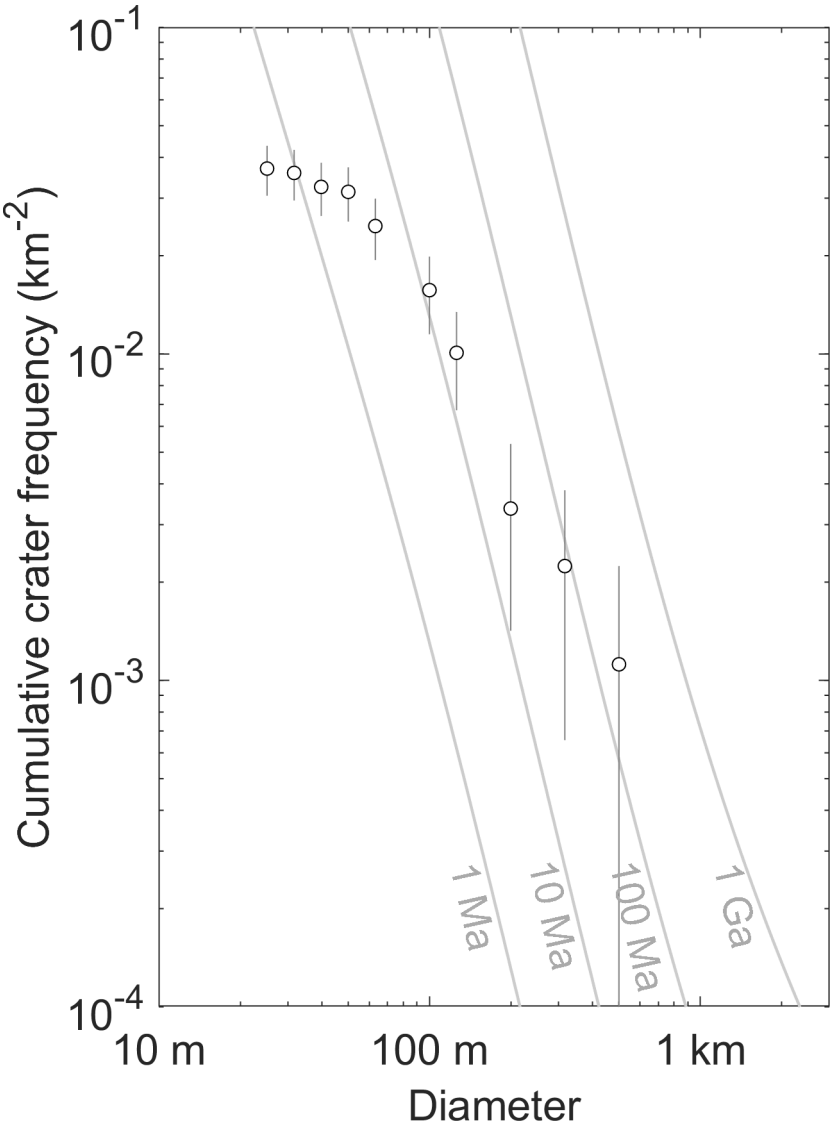

Fig. 15: Cumulative *CSFD* of the light-toned surface (area mapped as 'Lobate debris apron' in **Fig. 11a)** representing an area that is 893 km^2. A total of 33 craters were identified as unambiguously impact related based on size and morphology suggesting a crater retention age ~10 - ~100 Ma for craters D > 100 m.